Use of Electromagnetic and Acoustic Emission in Failure Monitoring of Cementitious Composites

Tomas Trcka [1,a], Pavel Koktavy [2,b] and Bohumil Koktavy [3,c]

[1,2] Brno University of Technology, Faculty of Electrical Engineering and Communication, Technicka 8, 616 00 Brno, Czech Republic.

[2] Brno University of Technology, Faculty of Civil Engineering, Zizkova 17, 602 00 Brno, Czech Republic.

[a] xtrcka03@stud.feec.vutbr.cz, [b] koktavy@feec.vutbr.cz, [c] koktavy.b@fce.vutbr.cz

Keywords: electromagnetic emission, acoustic emission, cracks, cementitious composites.

Abstract

This paper is focused on the failure monitoring in cementitious composites under mechanical loading. The aim was to determine how the cracks generation intensity depends on the aggregate size in tested concrete samples. Our diagnostic method is based on the measurement of electromagnetic and acoustic emission signals, which occur when the solid dielectric materials are mechanically stressed. Several groups of concrete samples with various concrete composition formulas have been prepared for our experiment. We made two-channel measurements of the concrete samples from each groups for defined loading conditions. This contribution describes our measurement system and also includes the pilot experimental results of the different cementitious specimens during linearly increasing uniaxial compression. From the obtained results can be concluded that the generated cracks intensity is significantly affected by the aggregate amount and size.

Introduction

When a solid is exposed to mechanical stress, emission of electrons, ions, ground state and excited neutrals, free radicals, electromagnetic emission in the frequency range from tenths of Hz up to the gamma radiation and acoustic emission may take place under certain conditions. This phenomenon is generally termed fractoemission. Fractoemission may be due to a several kinds of mechanical stress: tensile, compression, torsional stress. Furthermore, it may be induced by friction, shock, drilling, splitting, scaling, grinding, skimming etc [1, 2]. This phenomenon is particularly strong in composite materials. In the frequency domain are these processes characterized as a flicker noise especially in low frequency range. Several authors put forward physical interpretation directly connected with particular non-homogeneous structures [3].

Electromagnetic emission in the radio frequency region (EME) makes one of very important fractoemission components for the material research in physics as well as in engineering. In the past, great attention was paid to the application of EME from rocks and minerals being exposed to mechanical stress both in connection with earthquake and volcanic activity prediction and in the rock mechanics [4-6]. Although there are a number of experimental papers dealing with various EME aspects, the physical origin of this phenomenon is not sufficiently known for the time being.

Our diagnostic method designed for experimental examinations of EME signals in composite materials is based on an experimental fact, namely, that the formation of cracks in an electrically non-conducting material is accompanied by the generation of an electromagnetic field [7]. The

cracks generation in solids is accompanied by the redistribution of the electric charge. The crack walls are electrically charged and their vibrations produce time variable electrical dipole moments. Hence the individual cracks become electromagnetic field sources, which can be measured by appropriate sensors [7].
The signal of the acoustic emission (AE) is generated simultaneously with the EME signal. Acoustic emission appears due to release of elastic energy during this process and it is in frequency range of ultrasonic waves.
Electromagnetic emission and acoustic emission methods are promising methods to study the generation and behavior of cracks. The main advantage of EME and AE is their ability to be detected already in stressed stage, which prevents the macroscopic deterioration in solids. Suitably designed methodology of EME and AE signals measurement, processing and evaluation allows observing the response of stressed materials on applied mechanical load continuously and also allows obtaining the useful information about the processes taking place in the cracks formation in solids [7-9]. For the time being, the EME method is the only method suited to study the time development of the crack growth (crack propagation speed, crack face movement speed, crack length and size, etc.).

Measurement System

A fully automated set-up for EME and AE measurement (Fig.1) was developed in our laboratory. The main part of the measurement system is the adjustable hydraulic press which provides mechanical load of a sample in the range from 10 kN up to 100 kN. The press is controlled by computer via voltage that is set by card NI PCI-6014. Further, this card acquires the output voltage of Wheatstone bridge with a sensitive load cell which measures the mechanical load. A deformation meter is used to measure a sample contraction during compressive stress application. A change of the sample length is stored from the meter to computer by the RS-232 port.

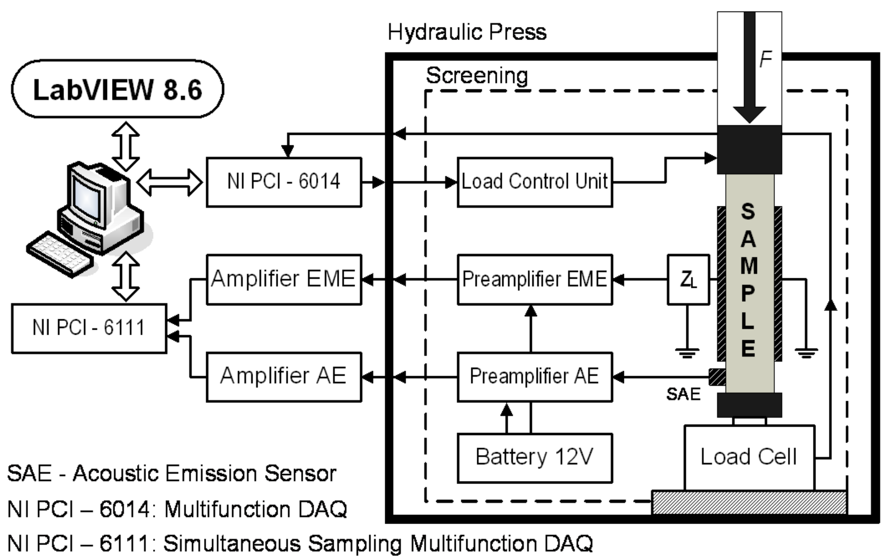

Fig.1. Experimental set-up.

EME and AE sensors. EME can be detected by either capacitance or inductive sensors. Capacitance sensors are well suited for studying small-sized rectangular or cylindrical specimens in the laboratory experiments, mainly due to their higher sensitivity and more appropriate transfer function [7]. For our measurements, the capacitance sensor is used to EME capture. In our experimental set-up, the capacitance sensor is formed by the specially made adjustable bracket with two electrodes, into which we can easily insert the rectangular samples from studied material.

The piezoelectric sensors from different vendors are used for AE monitoring. These sensors meet the requirements of the AE frequency band (at least up to 1 MHz) and are usually mounted by beeswax to a sample. This attachment provides good mechanical coupling between sample and sensor as well as easy mounting and removing of sensors.

EME and AE measurement channels. The EME channel consists of a capacitance sensor which dielectric is composed of the stressed sample, a high pass-filter-type load impedance ZL, a low-noise preamplifier PA31, and an amplifier AM22 with a set of filters. The total EME channel gain is 60 dB, the frequency range is from 30 kHz to 1.2 MHz and the sampling rate is of 5 MHz.
The AE channel consists of a piezoelectric acoustic sensor (30 kHz ~ 1 MHz), the low-noise preamplifier PA31 and the amplifier AM22 with a set of filters. The total AE channel gain is 40 dB, the frequency range is from 30 kHz to 1.2 MHz.

EME and AE Preamplifiers and Amplifiers. Preamplifier (3S SEDLAK PA31): This low-noise preamplifier exhibits the bandwidth from 20 Hz to 10 MHz, the high input impedance 10 MΩ/20 pF, the variable gain 6/20/40 dB and the noise voltage < 1,8 nV/√Hz.
Amplifier (3S SEDLAK AM22): This low-noise amplifier exhibits the bandwidth from 0.3 Hz to 1.2 MHz, set of high-pass and low pass filers, the input impedance 1 MΩ/50 pF and the noise voltage < 3 nV/√Hz.

EME and AE signals processing. Both signals of EME and AE are acquired by NI PCI 6111 card and stored to the PC, where further processing is carried out. Designed measurement system is controlled by the PC with software developed under the LabVIEW environment. The complex software package allows finding the typical events in the EME and AE channels and describing their fundamental parameters. Evaluation process of these parameters and measurement process are provided simultaneously (in real time).

Experimental Results

Our study in this paper is focused on cementitious composites. Several groups of concrete samples with various concrete composition formulas have been prepared for two-channel (EME and AE) measurement on our experimental set-up. The measured specimens were concrete blocks of overall dimensions 100 mm × 100mm × 80 mm. Test specimens were designed and manufactured according to R3 through R6 formulas, with following aggregate gradings:

- R3: sand (0-4) mm.
- R4: sand (0-4) mm, grit (4-8) mm.
- R5: sand (0-4) mm, grit (4-8) mm, (8-16) mm.
- R6: sand (0-4) mm, grit (4-8) mm, (8-16) mm, (16-22) mm.

Concrete blocks from each prepared groups were measured for defined loading conditions (linearly increasing uniaxial compression up to the load of 80 kN with a rate of 11 N/s.). The steel rods with a square cross-section of 8 × 8 mm were inserted between the specimens and the hydraulic press jaws. Figure 2 shows the example of the R5F specimens loading conditions, the curve of applied mechanical load and the histogram describing distribution of the fracture events (triggered by the AE signals) in time. Each bar in this chart describes number of AE events during the time interval of 60 s. Number of fracture events in individual time intervals is almost constant below the applied load of approximately 60 kN. The number of fracture events exponentially increases above this load level. The peek with the maximum value corresponds to the start of the whole sample destruction.

Figure 3 shows the example of measured signals which contain only separated EME and AE events. The time delay between both signals is caused by different propagation velocities of the acoustic and electromagnetic signals in the sample under examination. The AE signal time latency to the EME signal arrival provides information about the distance of the crack from the AE sensor. In case of the AE signal multi-channel measurement, we can get the useful information about the crack position in the stressed material [10,11]. Formation of the continuous EME and AE signals (see Fig.4) occurs just before the total destruction of the whole sample. In the case of R5F sample, the maximum load (before the sample destruction) was approximately 77 kN.

The curves of applied force versus sample deflection (contraction) for individual measured concrete samples are in figures 5-12. The histograms in these figures illustrate the distribution of AE (Fig.5,7,9,11) and EME (Fig.6,8,10,12) fracture events depending on the increasing sample contraction. Cumulative numbers of detected AE and EME events for defined applied force are in Fig.13 (AE) and Fig.14 (EME). Figure 15 shows the dependence of the total AE events number on the maximum aggregate size for defined mechanical load.

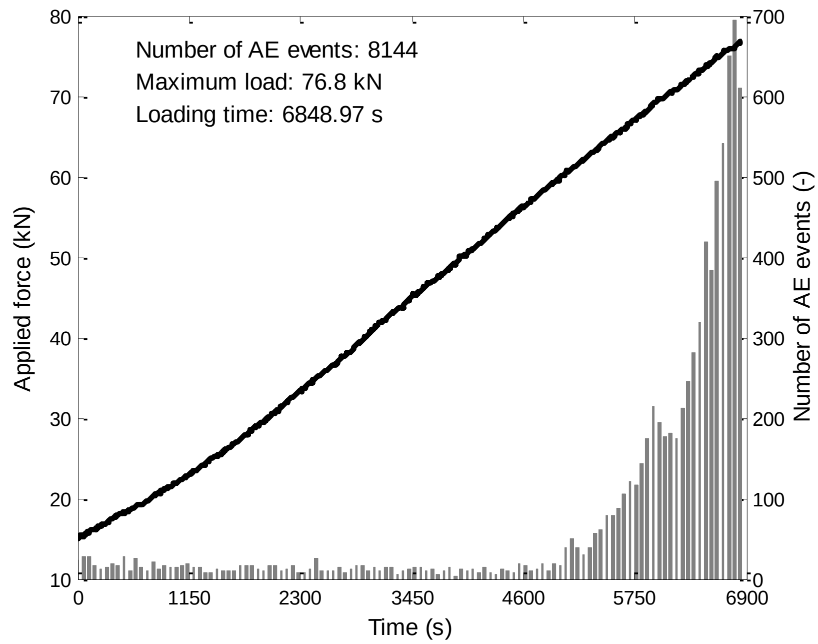

Fig.2. Applied mechanical load and the distribution of the fracture events (triggered by the AE signals) in time, sample R5F.

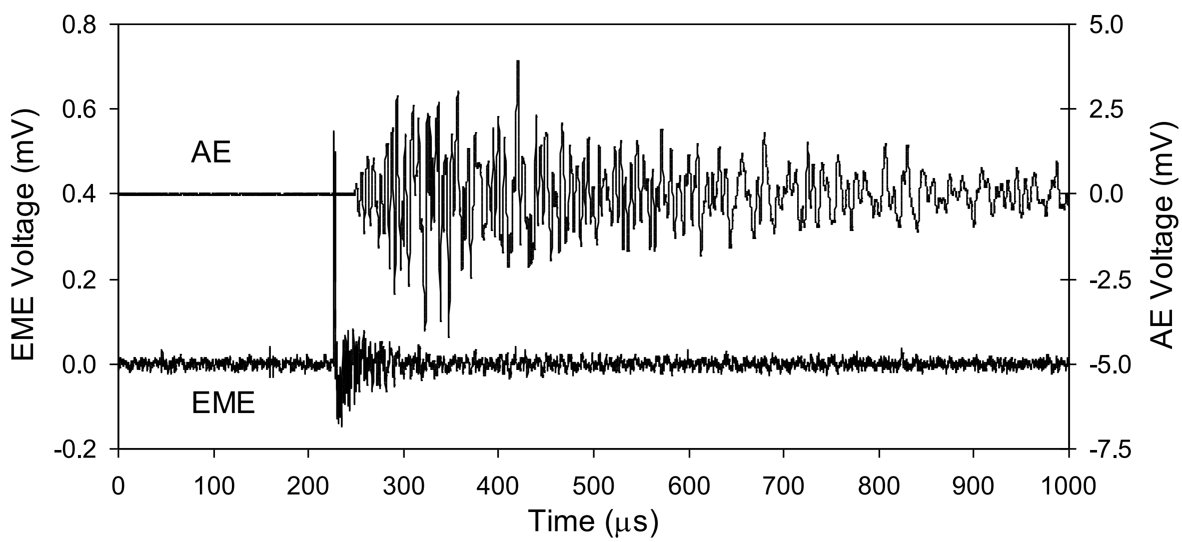

Fig.3. Separated EME and AE events, mechanical load 65.6 kN, sample R5F.

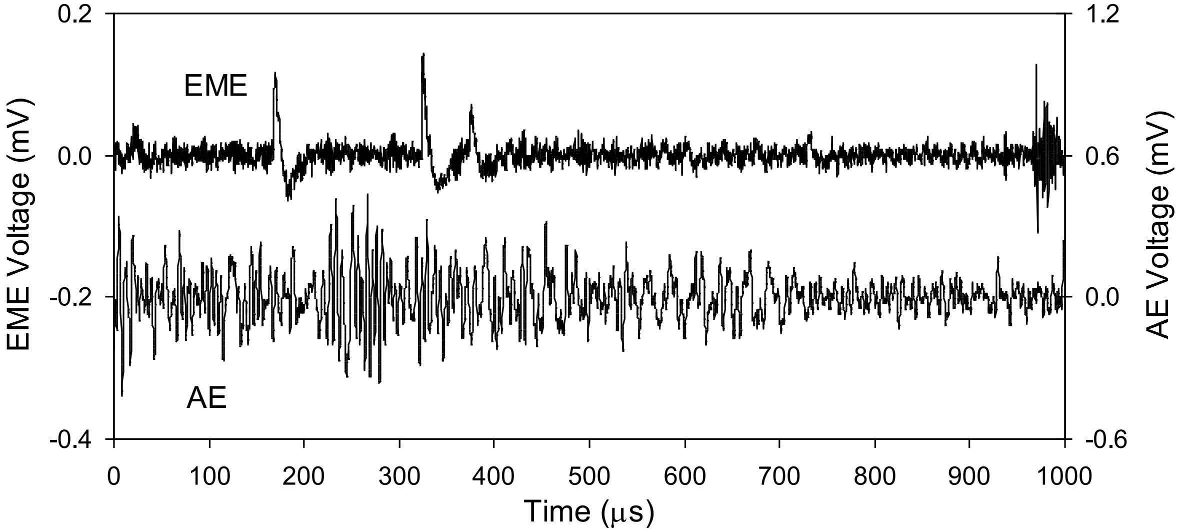

Fig.4. Continuous EME and AE events, mechanical load 76.8 kN, sample R5F.

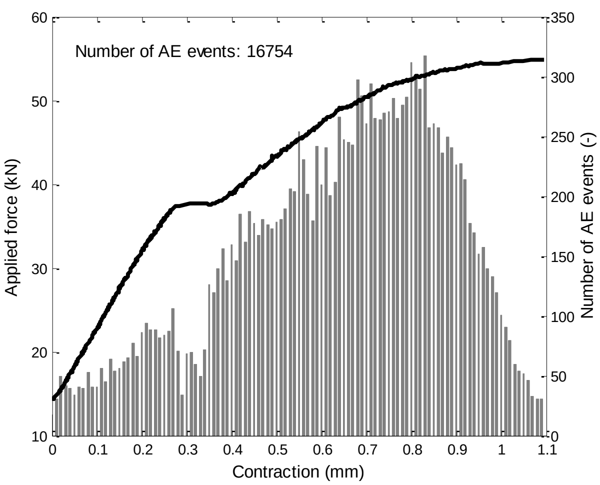

Fig.5. Sample R3D – AE intensity.

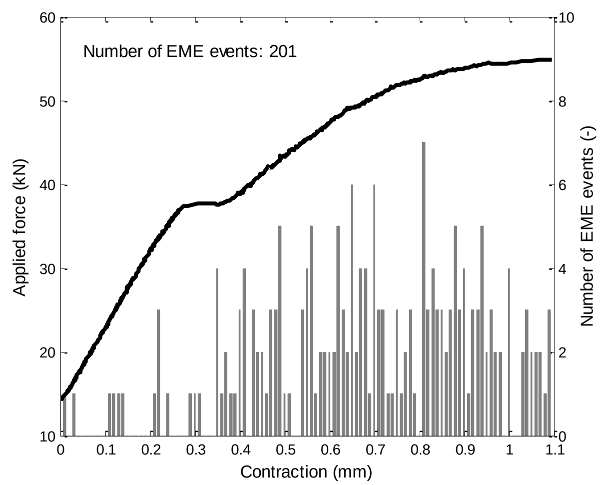

Fig.6. Sample R3D – EME intensity.

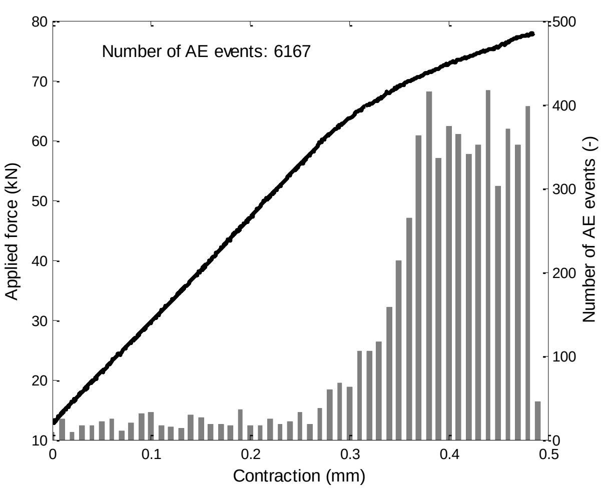

Fig.7. Sample R4A – AE intensity.

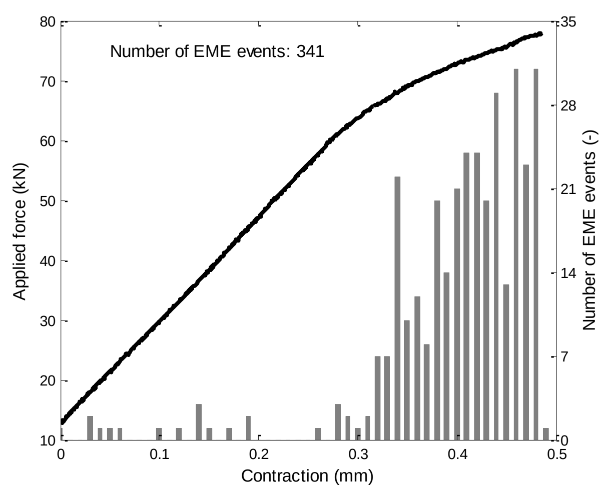

Fig.8. Sample R4A – EME intensity.

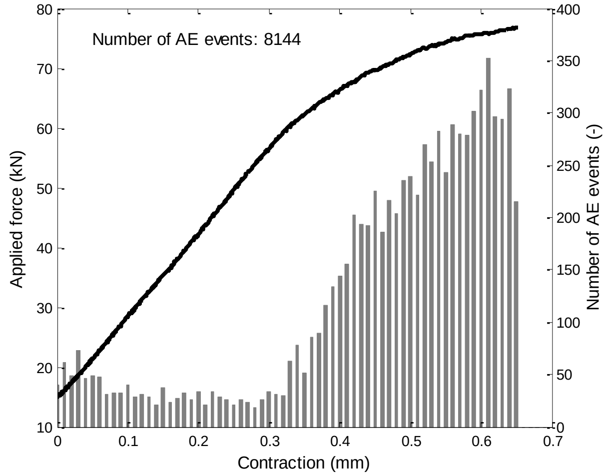

Fig.9. Sample R5F – AE intensity.

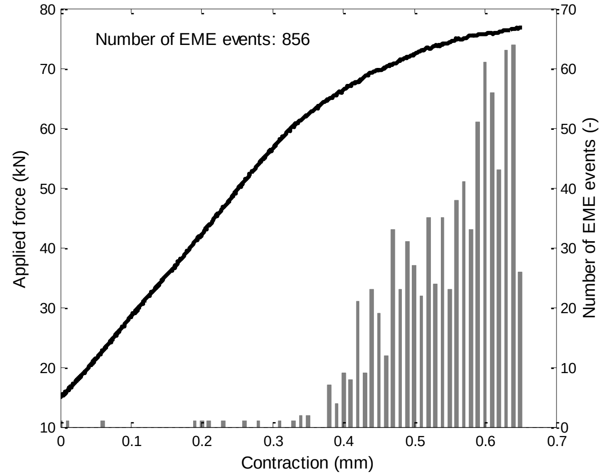

Fig.10. Sample R5F – EME intensity.

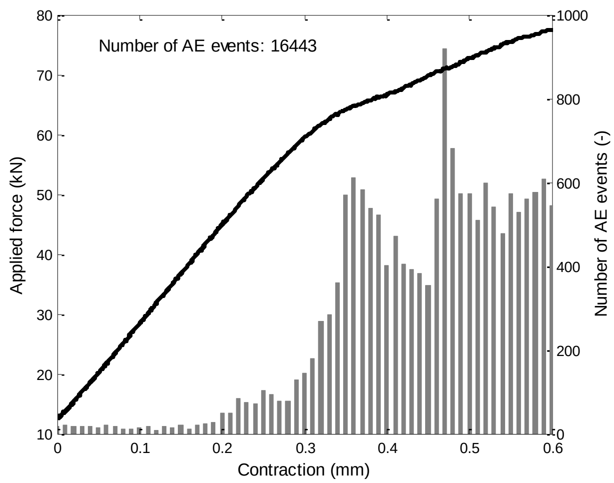

Fig.11. Sample R6D – AE intensity.

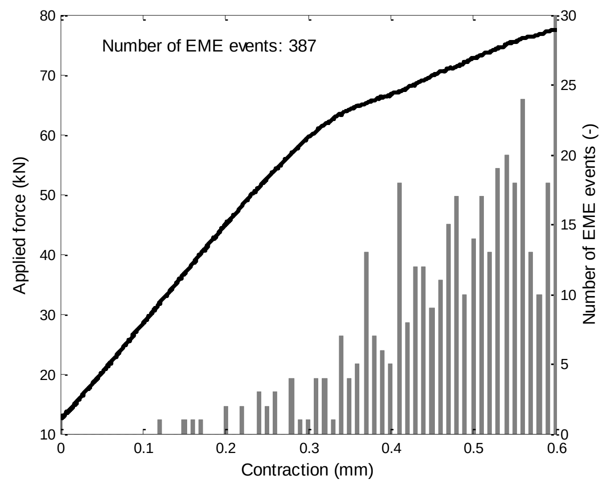

Fig.12. Sample R6D – EME intensity.

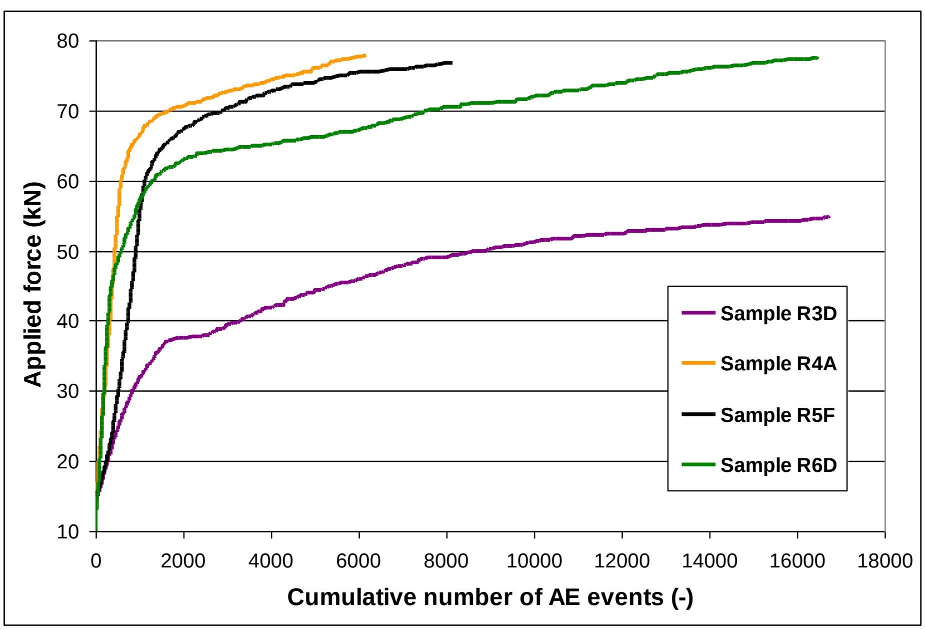

Fig.13. Cumulative numbers of detected AE events for defined applied force.

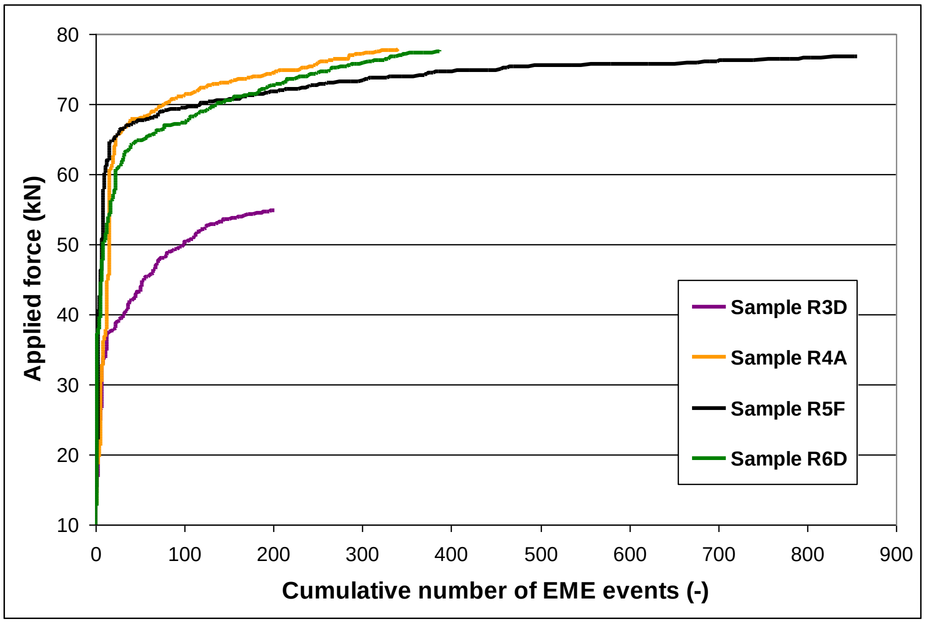

Fig.14. Cumulative numbers of detected EME events for defined applied force.

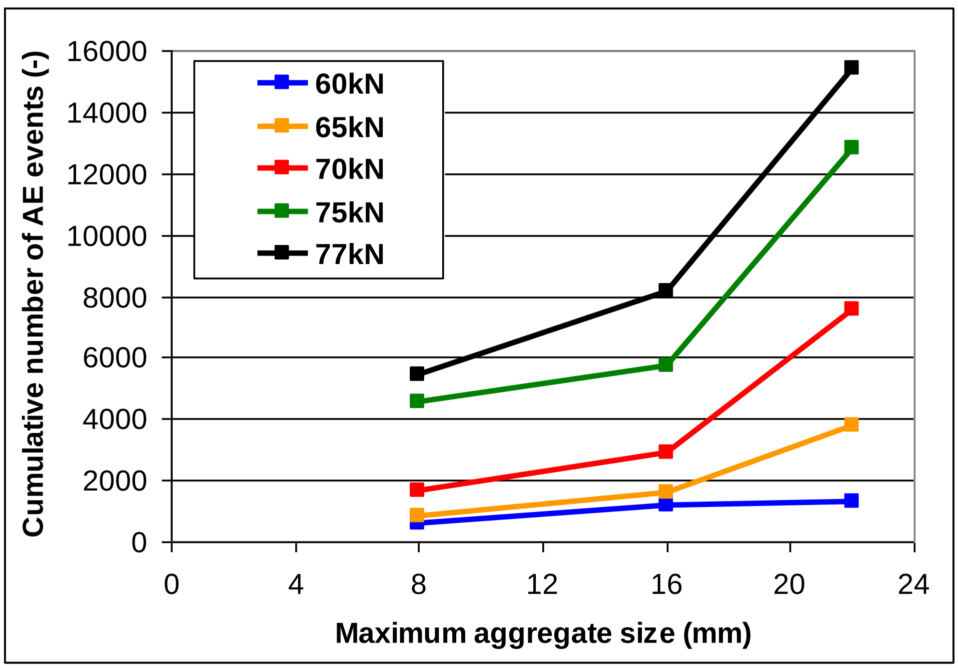

Fig.15. Dependence of the total AE events number on the maximum aggregate size for defined mechanical load.

Conclusion

For the R3 sample is evident that the intensity of detected AE signals increases from the beginning of mechanical loading (Fig.5) and the cumulative number of AE events for defined load reaches significantly higher values compared to the rest of the samples. This is valid only to mechanical load approximately 53 kN during which the R3D sample was destroyed (see Fig.13) due to low strength of R3-type samples manufactured formula. The addition of aggregate with larger maximum size (4-8 mm) led to growth of the loaded samples maximum strength and the total number of detected

AE signals was distinctly reduced (see R4A sample in Fig.13). It is surprising that the followed addition of fraction with the larger grain size increased the detected AE signals frequency. From the cumulative number of AE events (Fig.13) can be plotted the dependence of the total AE events number on the maximum aggregate size for defined mechanical load (see Fig.15).

In the case of electromagnetic emission was the largest detected EME signals intensity (at low values of mechanical load) again for samples with R3 manufactured formula (Fig.14) and the total detected EME events number of R4A, R5F and R6D samples was greater in comparison with the R3D sample.

From the obtained results can be concluded that the generated cracks intensity is significantly affected by the aggregate amount and size. For more detailed studies will be performed additional measurements on a larger number of concrete samples with defined composition formulas.

Acknowledgements

This research has been supported by the Brno BUT Specific Research FEKT-S-11-11, by the Grant Agency of the Czech Republic within the framework of the projects 102/09/H074 "*Diagnostics of material defects using the latest defectoscopic methods*" and P104/11/0734 "*Utilization of electromagnetic and acoustic emission in research of advanced composite materials for structural applications*". This support is gratefully acknowledged.

References

[1] J.T. Dickinson, M.K. Park, E.E. Donaldson and L.C. Jensen: J. Vac. Sci. Technol Vol. 20 (3) 436-9 (1982).
[2] J.T. Dickinson, E.E. Donaldson and M.K. Park: J. Mater. Sci. 16 (10) 2897-908 (1981).
[3] R. Macku, P. Koktavy: Physica status solidi Vol. 207(10). p. 2387 – 2394 (2010).
[4] V. Hadjicontis, G.S. Tombras, D. Ninos and C. Mavromatou: IEEE Geoscience and Remote Sensing Letters 2(2) 118–20.
[5] Y. Mori, K. Sato, Y. Obata and K. Mogi: Proc. Progress in Acoustic Emission IX (1998), pp II-1 – II-8.
[6] P. Koktavy, J. Pavelka and J. Sikula: Meas. Sci. Technol. Vol. 15 (1) 973 – 7 (2004).
[7] P. Koktavy: Measurement Science and Technology Vol. 20(1). p. 0-7 (2008).
[8] P. Koktavy, T. Trcka, B. Koktavy: In 21st International Conference on Noise and Fluctuations ICNF 2011. Toronto, Kanada, IEEE. p. 88 – 91 (2011).
[9] T. Trcka, P. Koktavy, P. Tofel: Key Engineering Materials Vol. 465(1). p. 332 – 335 (2011).
[10] P. Sedlak, Y. Hirose, S. Khan, M. Enoki and J. Sikula: Ultrasonics Vol. 49 (2), p. 254-262 (2009).
[11] P. Sedlak, J. Sikula, T. Lokajicek and Y. Mori: Measurement Science and Technology Vol. 19 (4) 0-045701 (2008).